Electronic Supplementary Information

Stable Bimetal-MOF Ultrathin Nanosheets for Pseudocapacitors with Enhanced performance

Hai-Meng Ma[†,‡,#], Jing-Wei Yi[†,#], Shuang Li[†,*], Chong Jiang[†], Jun-Hua Wei[†], Ya-Pan Wu[†], Jun Zhao[†] and Dong-Sheng Li[†,§,*]

[†]College of Materials and Chemical Engineering, Key Laboratory of Inorganic Nonmetallic Crystalline and Energy Conversion Materials, China Three Gorges University, Yichang, 443002, P. R. China

[‡]College of Electrical Engineering & New Engery, China Three Gorges University, Yichang, 443002, P. R. China.

[§]State Key Laboratory of Structural Chemistry, Chinese Academy of Sciences, Fujian, Fuzhou 350002, PR China

*E-mail: lishmail@126.com

*E-mail: lidongshengl@126.com.

S1. Experimental section

Materials

All reagents and solvents were commercially available and used as received without further purification.

Synthesis of NiCo-BDC nanosheets

The NiCo-BDC nanosheets were synthesized by a modification of the method previously reported.[1] In a typical procedure, $NiCl_2 \cdot 6H_2O$, $CoCl_2 \cdot 6H_2O$ and BDC in a molar ratio 1:1:2 were dissolved in the 16:1:1 mixture of DMF, ethanol and water under vigorous stirring to form a homogeneous solution. After being stirred for 30 min, the solution was transferred into a 40 mL Teflon-lined stainless steel vessel and maintained at 140℃ for 2 days. Then the reaction system was allowed to cool down to room temperature naturally. Finally, the obtained products were collected by centrifugation,

washed with DMF, water and ethanol for several times, and then dried at 60℃ overnight under vacuum.

Synthesis of NiMn-BDC nanosheets

The NiMn-BDC nanosheets were synthesized by the similar manner of NiCo-BDC nanosheets, except that the molar ratio of $NiCl_2 \cdot 6H_2O$, $MnCl_2 \cdot 6H_2O$ and BDC was 1:2:2.

Synthesis of Ni-BDC, Co-BDC and Mn-BDC nanosheets

The preparation process was same as that of NiCo-BDC nanosheets or NiMn-BDC nanosheets without the addition of $CoCl_2 \cdot 6H_2O$ and $NiCl_2 \cdot 6H_2O$, respectively.

Electrochemical measurements

All the electrochemical measurements were carried out with an electrochemical workstation (CHI 660E) using a standard three-electrode measurement in 1 M KOH aqueous solution. The platinum electrode was used as the counter electrode and Hg/HgO was used as the reference electrode. The working electrode was prepared by mixing 85 wt% active material, 10 wt% acetylene black and 5 wt% polytetrafluoroethylene (PTFE) binder with a few drops of ethanol to form a homogenous slurry. The slurry was coated on the nickel foam current collector of about 2 cm^2 (1*2 cm), then pressed at 10 MPa and further dried at 80℃ overnight under vacuum. The loading densities of active materials on nickel foam were about 4 mg cm^{-2} for all electrodes. Cyclic voltammetry (CV) curves were recorded between 0.1 and 0.6 V (*vs.* Hg/HgO) at scan rates of 10, 20, 50 and 100 mV s^{-1}, respectively. Galvanostatic charge-discharge tests were obtained in the potential between 0.1 and 0.55 V (*vs.* Hg/HgO) at current densities from 0.5 to 5 A g^{-1}. The specific capacitances ($C_{s)}$ of the samples were calculated based on the charge/discharge curves.

Characterization

X-ray diffraction (XRD) was performed on a Rigaku Ultima IV diffractmeter with Cu Kα radiation (λ=1.5406 Å). The transmission electron microscopy (TEM) image was carried out on a JEM-2100F field emission electron microscope at an acceleration voltage of 200 kV. High-angle annular dark-field scanning transmission spectroscopy (HAADF-STEM) image and corresponding energy-dispersive spectroscopy (EDS)

mapping analyses were performed on a JEOL JEM-ARF 200F TEM/STEM with a spherical aberration corrector. The field emission scanning electron microscopy (FE-SEM) images were taken on a JEOL JSM-6700F SEM. X-ray photoelectron spectra (XPS) was acquired on an ESCALAB MK Ⅱ with Mg Kα as the excitation source. X-ray absorption near-edge structure (XANES) measurements were conducted on the X-ray Magnetic Circular Dichroism End-station at Hefei Synchrotron Radiation Facility in the University of Science of Technology of China. FT-IR spectra (KBr pellets) were conducted on a Thermo Electron NEXUS 670 FTIR spectrometer. The inductively coupled plasma (ICP) emission spectra were carried out on a Perkin Elmer Optima 7300DV ICP emission spectroscope.

S2. Additional characterization information

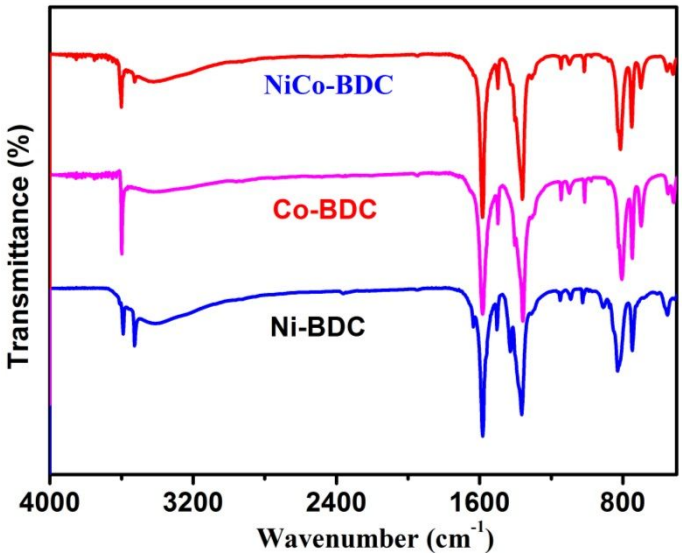

Figure S1. FT-IR spectra of NiCo-BDC, Co-BDC and Ni-BDC.

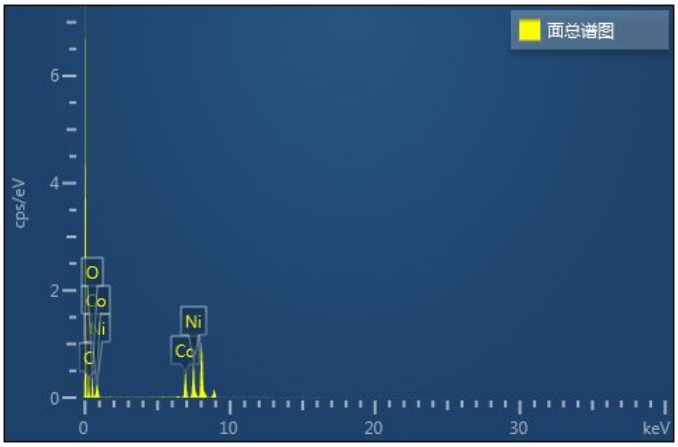

Figure S2. EDS spectrum of the NiCo-BDC ultrathin nanosheets. From the EDS measurement, Ni, Co, C and O are the only elements composing of the nanosheet.

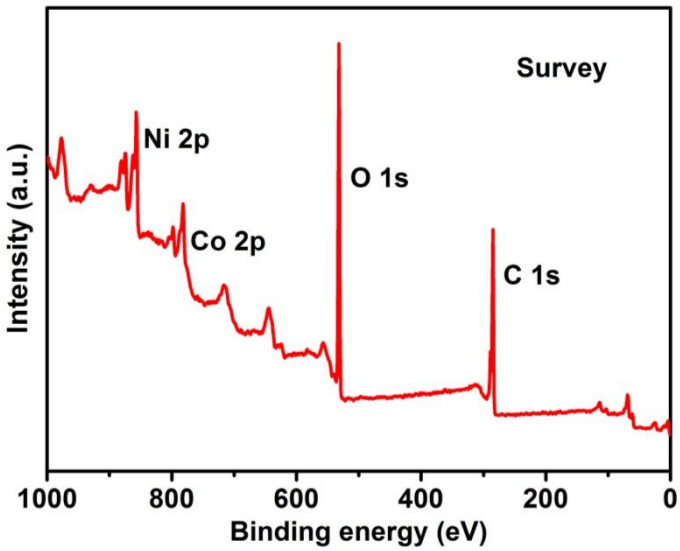

Figure S3. XPS spectrum of the survey of the ultrathin NiCo-BDC nanosheets.

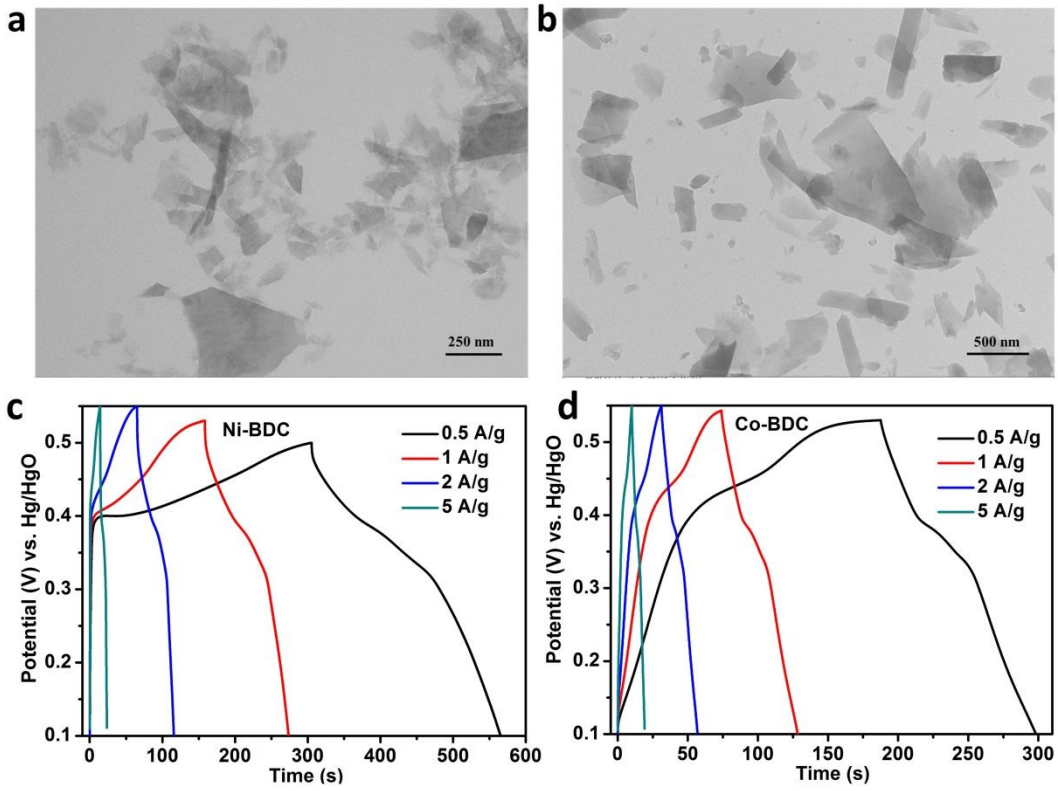

Figure S4. TEM images of (a) Ni-BDC and (b) Co-BDC. Galvanostatic charge-discharge curves of the Ni-BDC (c) and Co-BDC (d) at various current densities (from 0.5 A/g to 5 A/g).

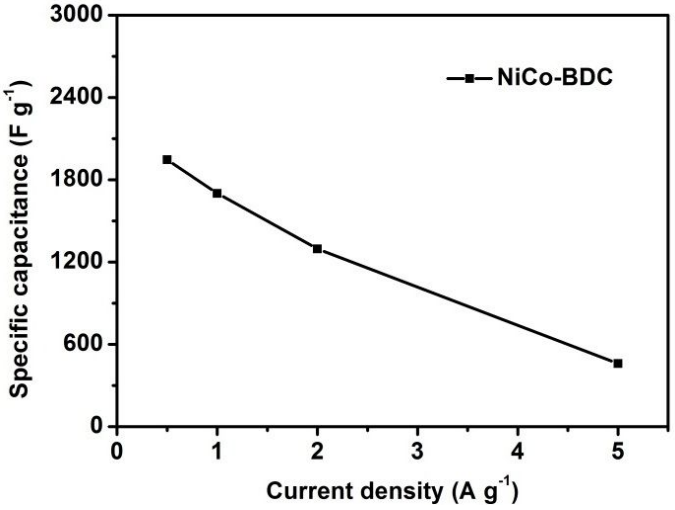

Figure S5. The specific capacitances of the NiCo-BDC nanosheets at different current densities.

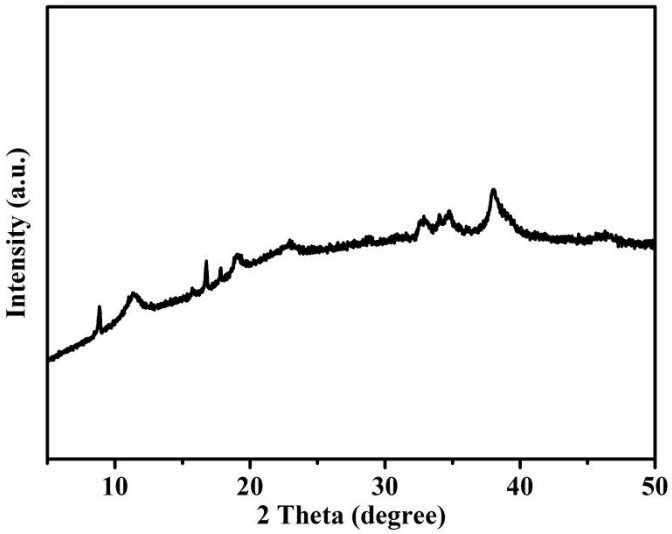

Figure S6. The XRD pattern of NiCo-BDC nanosheets after the alkaline treatment in 1 M KOH for 12 h.

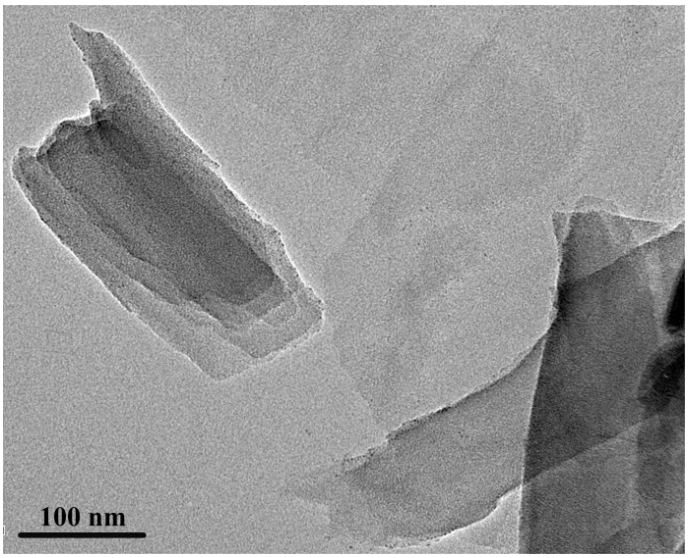

Figure S7. TEM image of the NiCo-BDC nanosheets after stability test.

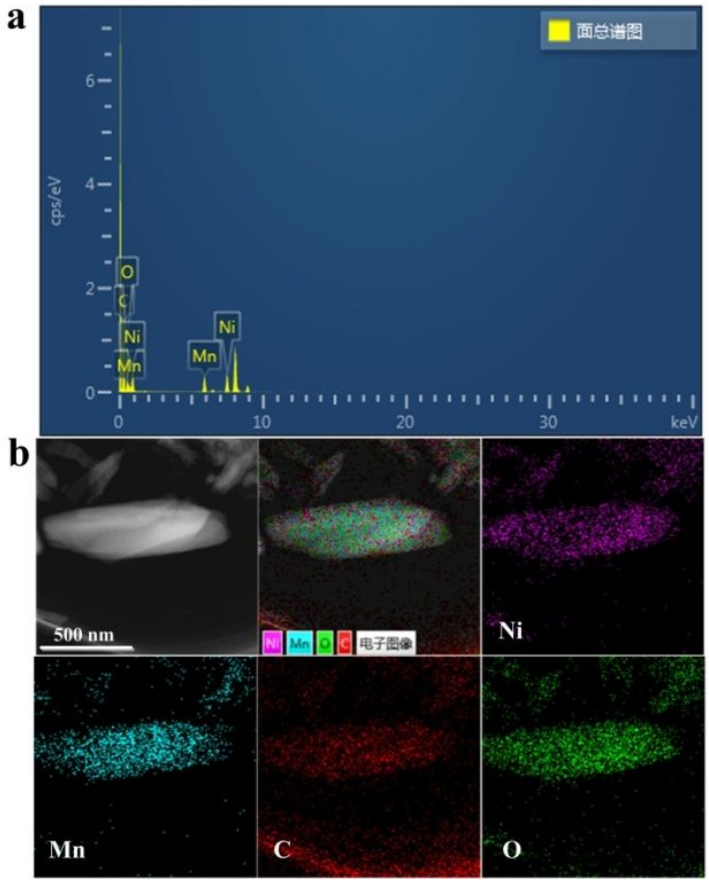

Figure S8. (a) EDS spectrum of the NiMn-BDC ultrathin nanosheets. (b) Element mapping images of the NiMn-BDC ultrathin nanosheets.

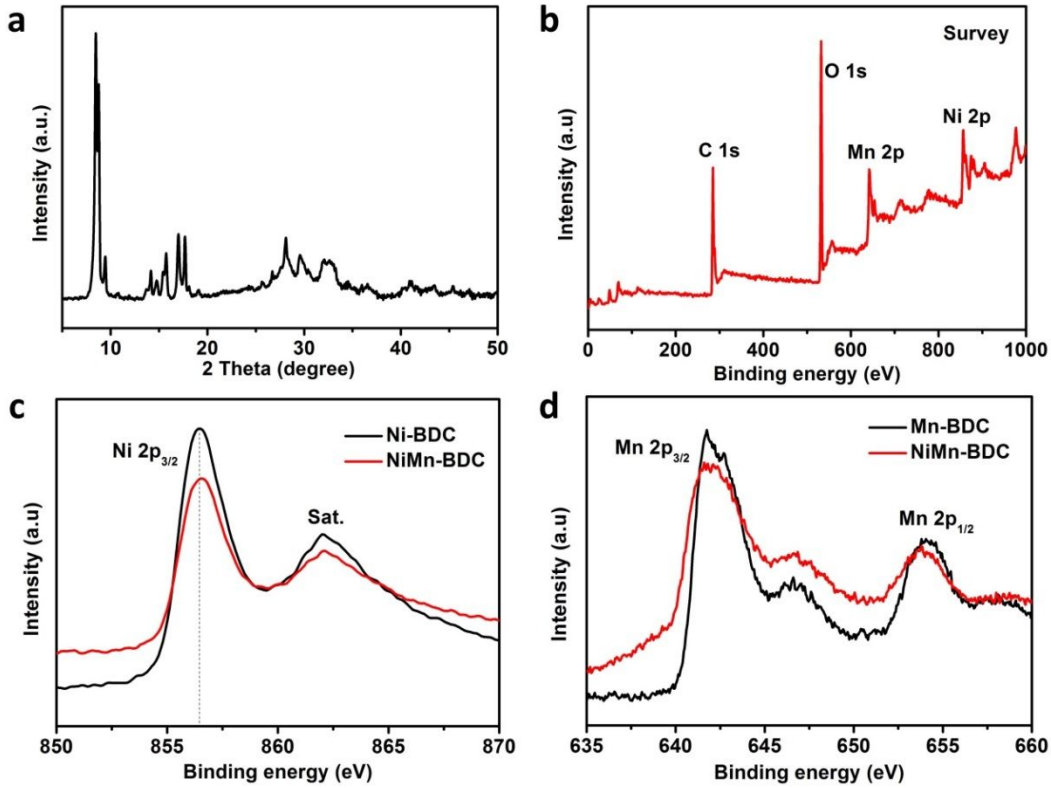

Figure S9. (a) XRD pattern of the NiMn-BDC. XPS spectra of (b) the survey spectrum of NiMn-BDC; (c) Ni $2p_{3/2}$ of Ni-BDC and NiMn-BDC; (d) Mn 2p of Mn-BDC and NiMn-BDC.

Table S1. Comparison of the specific capacitances of present work and the other electrode materials in a three-electrode system.

Materials	Electrolyte solution	Current collector	Test Condition	Specific Capacitance (F g^{-1})	Ref.
NiCo-BDC	1.0 M KOH	Ni foam	0.5 A g^{-1}	1945.83	This work
			1 A g^{-1}	1700.40	
Ni/Co-MOF	1.0 M LiOH	Glassy carbon disk	0.5 A g^{-1}	530.4	2
Co-MOF	1.0 M LiOH	Ni foam	0.5 A g^{-1}	230.5	3
Ni-MOF	4.0 M KOH	Ni foam	1 A g^{-1}	552	4
Ni-MOF	2.0 M KOH	Ni foam	1 A g^{-1}	726	5
Ni-MOF	3.0 M KOH	Ni foam	1.4 A g^{-1}	988	6
Ni-MOF	6.0 M KOH	Stainless steel mesh	0.5 A g^{-1}	1127	7
Zn-doped Ni-MOF	6.0 M KOH	Stainless steel mesh	0.25 A g^{-1}	1620	8
Ni/Co-MOF	3.0 M KOH	Stainless steel grid	1 A g^{-1}	1049	9
Ni-Co-S/G	6.0 M KOH	Ni foam	1 A g^{-1}	1492	10
H-NiOOH/GS	2.0 M KOH	Ni foam	1 A g^{-1}	1162	11
$NiCo_2O_4$@Ni WO_4	6.0 M KOH	Ni foam	1 A g^{-1}	1384	12
$NiCo_2O_4$@Mn O_2	1.0 M KOH	Ni foam	1 A g^{-1}	913.6	13

References

1. S. Zhao, Y. Wang, J. Dong, C. T. He, H. Yin, P. An, K. Zhao, X. Zhang, C. Gao, L. Zhang, J. Wang, J. Zhang, A. M. Khattak, N. A. Khan, Z. Wei, J. Zhang, S. Liu, H. Zhao and Z. Tang, *Nat. Energy.,* 2016, **1**, 16184.
2. H. Xia, J. Zhang, Z. Yang, S. Guo, S. Guo and Q. Xu, *Nano-Micro Lett.,* 2017, **9**, 43.
3. H. Yu, D. Xu and Q. Xu, *Chem. Commun.,* 2015, **51**, 13197.
4. C. Qu, Y. Jiao, B. Zhao, D. Chen, R. Zou, K. S. Walton and M. Liu, *Nano Energy*, 2016, **26**, 66.

5. L. Kang, S-X. Sun, L-B. Kong, J-W. Lang, Y-C. Luo, *Chin. Chem. Lett.*, 2014, **25**, 957.
6. Y. Yan, P. Gu, S. Zheng, M. Zheng, H. Pang and H. Xue, *J. Mater. Chem. A.,* 2016, **4**, 19078.
7. J. Yang, P. Xiong, C. Zheng, H. Qiu and M. Wei, *J. Mater. Chem. A.*, 2014, **2**, 16640.
8. J. Yang, C. Zheng, P. Xiong, Y. Li and M. Wei, *J. Mater. Chem. A.*, 2014, **2**, 19005.
9. H. G-Ranjbar, M. Soleimani and H. R. Nader, *New J. Chem.,* 2016, **40**, 9187.
10. J. Yang, C. Yu, X. Fan, S. Liang, S. Li, H. Huang, Z. Ling, C. Hao and J. Qiu, *Energy Environ. Sci,.* 2016, **9**, 1299.
11. R. Wang, C. Xu and J-M. Lee, *Nano Energy,* 2016, **19**, 210.
12. S. Chena, G. Yanga, Y. Jiab, H. Zheng, *J. Mater. Chem. A.,* 2017, **5**, 1028.
13. Y. Zhang, B. Wang, F. Liu, J. Cheng, X. Zhang, L. Zhang, *Nano Energy,* 2016, **27**, 627.